The Journal of Immunology

STAT-1 Signaling in Human Lung Fibroblasts Is Induced by Vanadium Pentoxide through an IFN-β Autocrine Loop

Aurita Antao-Menezes, Elizabeth A. Turpin, Phillip C. Bost, Jessica P. Ryman-Rasmussen and James C. Bonner

J Immunol 2008; 180:4200-4207; ;
doi: 10.4049/jimmunol.180.6.4200
http://www.jimmunol.org/content/180/6/4200

The Journal of Immunology is published twice each month by
The American Association of Immunologists, Inc.,
1451 Rockville Pike, Suite 650, Rockville, MD 20852

Print ISSN: 0022-1767 Online ISSN: 1550-6606.

STAT-1 Signaling in Human Lung Fibroblasts Is Induced by Vanadium Pentoxide through an IFN-β Autocrine Loop[1]

Aurita Antao-Menezes,* Elizabeth A. Turpin,* Phillip C. Bost,† Jessica P. Ryman-Rasmussen,*† and James C. Bonner[2]*†

The inhalation of vanadium pentoxide (V_2O_5) results in bronchitis and airway fibrosis. The lung fibrotic response to V_2O_5 partially resolves where fibroblasts first proliferate and deposit collagen, but then undergo growth arrest and apoptosis. STAT-1 mediates fibroblast growth arrest and apoptosis. We previously reported that STAT-1 is a protective factor and mice lacking STAT-1 are more susceptible to lung fibrosis. We also reported that V_2O_5-induced STAT-1 phosphorylation in lung fibroblasts requires H_2O_2 and de novo protein synthesis. In this study, we identified IFN-β as the protein that mediates STAT-1 activation by V_2O_5 in normal human lung fibroblasts and identified NADPH and xanthine oxidase systems as sources of H_2O_2 that drive *IFN-β* gene expression. STAT-1 phosphorylation was decreased with neutralizing Abs to IFN-β as well as an inhibitor of JAK. V_2O_5 also increased transcription of an IFN-inducible and STAT-1-dependent chemokine, CXCL10. Inhibition of H_2O_2-generating enzyme systems NADPH oxidase by apocynin and xanthine oxidase by allopurinol individually reduced STAT-1 phosphorylation. Apocynin and allopurinol also decreased V_2O_5-induced IFN-β mRNA levels and CXCL10 expression. IFN-α transcription was inhibited only by allopurinol. Taken together, these data indicate that fibroblasts play a role in the innate immune response to vanadium-induced oxidative stress by synthesizing IFN-β and activating STAT-1 to cause growth arrest and increase levels of CXCL10, a potent antifibrotic factor. This mechanism is postulated to counterbalance profibrogenic mechanisms that follow V_2O_5 injury. *The Journal of Immunology,* 2008, 180: 4200–4207.

Vanadium pentoxide (V_2O_5) is commonly released during the burning of fuel oil and is a cause of chronic bronchitis for workers in the petrochemical industry (1, 2). The disease pathology after V_2O_5 exposure in rodents includes mucous cell metaplasia, lymphocyte infiltration, fibroblast hyperplasia, and airway fibrosis (3). Fibroblasts play a central role in mediating fibrosis by migrating to sites of injury, proliferating, and secreting collagen to form scar tissue (4). Fibroblasts further participate in either the amplification or resolution of a fibrotic response by secreting a variety of soluble factors (e.g., growth factors, cytokines, chemokines) (5). Although much is known about profibrotic factors released by fibroblasts and other pulmonary cell types, the mechanisms that mediate fibroblast growth arrest and apoptosis which lead to the resolution of fibrosis are not well-understood.

STAT-1 mediates growth arrest and apoptosis in response to cytokines and oxidative stress (6, 7). STAT-1 acts in opposition to the proliferative activity of STAT-3, which is activated by growth factors such as epidermal growth factor (EGF)[3] and platelet-derived growth factor (PDGF) (8). We recently reported that STAT-1 also acts in opposition to the stimulatory action of STAT-6 in promoting *PDGF* gene expression in response to IL-13 (9). Moreover, we discovered that mice deficient in STAT-1 have increased susceptibility to bleomycin-induced lung fibrosis, indicating that STAT-1 plays a protective role during fibrogenesis (10). Finally, we showed that V_2O_5 is a potent activator of STAT-1 in lung fibroblasts (11). Therefore, the evidence suggests that STAT-1 contributes to the resolution of V_2O_5-induced fibrosis.

V_2O_5-induced STAT-1 phosphorylation in fibroblasts is mediated by H_2O_2. The membrane bound NADPH oxidase (12, 13) and cytoplasmic xanthine oxidase are primary sources of H_2O_2 (14). We previously reported that V_2O_5-induced STAT-1 phosphorylation is blocked by catalase (an H_2O_2 scavenger) and exogenous H_2O_2 added to fibroblasts activates STAT-1 (11). However, in contrast to H_2O_2-induced STAT-1 activation which occurs within minutes after exposure, V_2O_5-induced STAT-1 activation occurs after 12 h (11). This delayed temporal pattern of STAT-1 activation also corresponds to the release of micromolar levels of H_2O_2 by fibroblasts (15). Moreover, V_2O_5-induced STAT-1 activation is blocked by cycloheximide, indicating a requirement for de novo protein synthesis (11). However, the protein(s) that mediated V_2O_5-induced STAT-1 activation in a H_2O_2-dependent manner were not identified in these studies.

In the present study, we identified IFN-β as the protein that mediates STAT-1 activation by V_2O_5. Increased *IFN-β* gene expression induced by V_2O_5 and consequent STAT-1 activation were significantly reduced by NADPH oxidase inhibitors apocynin and diphenyliodonium chloride (DPI) as well as the xanthine oxidase inhibitor allopurinol. These findings indicate a requirement for dual H_2O_2-generating enzyme systems. In addition, IFN-inducible chemokine CXCL10 (inducible protein-10) mRNA and protein

*The Hamner Institutes for Health Sciences, Research Triangle Park, NC 27709; and †Department of Environmental and Molecular Toxicology, North Carolina State University, Raleigh, NC 27695

Received for publication July 18, 2007. Accepted for publication January 16, 2008.

The costs of publication of this article were defrayed in part by the payment of page charges. This article must therefore be hereby marked *advertisement* in accordance with 18 U.S.C. Section 1734 solely to indicate this fact.

[1] This work was supported by The Long-Range Research Initiative of the American Chemistry Council and National Institutes of Health R21-ES015801-01.

[2] Address correspondence and reprint requests to Dr. James C. Bonner, North Carolina State University, Raleigh, NC 27695. E-mail address: james_bonner@ncsu.edu

[3] Abbreviations used in this paper: EGF, epidermal growth factor; PDGF, platelet-derived growth factor; DPI, diphenyliodonium chloride; SFDM, serum-free defined medium; CM-H_2DCFDA, 5-(and-6)-chloromethyl-2′,7′dichlorodihydrofluorescein diacetate, acetyl ester; RT, reverse transcriptase; ROS, reactive oxygen species; CTGF, connective tissue growth factor; HB-EGF, heparin-binding EGF.

levels were increased by V_2O_5 and blocked by apocynin, allopurinol, or DPI. Our findings suggest a novel mechanism whereby V_2O_5-induced oxidative stress stimulates an innate immune response involving autocrine IFN-β that could mediate the resolution of fibrotic lesions via activation of STAT-1.

Materials and Methods

Reagents

V_2O_5 was purchased from Sigma-Aldrich. H_2O_2 was obtained from Fisher-Scientific. Total STAT-1 Ab and phospho-STAT-1 (Tyr^{701}) Ab that detects phosphorylated tyrosine 701 of p91 STAT-1 were purchased from New England Biolabs. DPI, apocynin, and allopurinol were purchased from Sigma-Aldrich. The JAK inhibitor JAK I InSolution was purchased from Calbiochem. Neutralizing polyclonal Abs to human IFN-α and IFN-β were purchased from R&D Systems. 5-(and-6)-chloromethyl-2′,7′dichlorodihydrofluorescein diacetate, acetyl ester (CM-H_2DCFDA) was obtained from Invitrogen Life Technologies.

Cells

Three different normal diploid human lung fibroblasts (CCD-16Lu, CCD-19Lu, CCD-11Lu) were purchased from American Type Culture Collection (ATCC) and were originally obtained by autopsy from individuals differing in age, sex, and ethnic background. More detailed information on these lung fibroblasts can be obtained from the ATCC website (www.atcc.org). For most experiments, HLF 16Lu were used due to our previous work with these cells in elucidating mechanisms of vanadium-induced cell signaling and gene expression (15–17). Selected experiments compared all three different human lung fibroblast isolates.

Measurement of intracellular H_2O_2

Confluent monolayers of human lung fibroblasts were rendered quiescent in serum-free defined medium (SFDM; Ham's F12, 0.25% BSA, 1 g/L insulin, 0.55 g/L transferrin, 0.67 mg/L sodium selenite and antibiotic-antimycotic) for 24 h. Cells were either left untreated in SFDM or treated with V_2O_5 (10 μg/cm^2). At the end of each indicated treatment period, cells were washed with PBS. To incorporate the dye, cells were loaded with 10 μM CM-H_2DCFDA or left untreated (for background subtraction) for 45 min at 37°C. Unincorporated dye was removed by washing with PBS and then cells were allowed to recover for a further 30 min in medium at 37°C. Cells were washed again in PBS and equal number of cells were loaded on a fluorescence plate reader and read at excitation wavelength 485 nm and emission wavelength 538 nm. After background subtraction, fluorescence values were compared with time-matched cells that did not receive V_2O_5 and the ratio obtained was expressed as fold change over control.

Measurement of extracellular H_2O_2

Extracellular H_2O_2 was measured using the Amplex Red assay kit (catalog no. A22188; Molecular Probes). Confluent cultures of human lung fibroblasts were rendered quiescent in SFDM for 24 h before treatment with V_2O_5. Aliquots of the medium were collected at various times post-V_2O_5 exposure. H_2O_2 was detected by loading 100 μl of the cell supernatant in a microtiter plate and incubated for 30 min at 25°C (protected from light) in the presence of phosphate buffer containing 400 μl of Amplex Red reagent and 2 U/ml HRP. Fluorescence was read at 590 nm and background fluorescence was corrected by subtracting the values derived from medium alone (no cells). Because reducing agents present in the medium could lead to some background fluorescence, catalase was added to parallel wells in all experiments to ensure that the fluorescence detected was due to the presence of H_2O_2. All measurements were made in duplicate dishes at each time point, and three different aliquots collected from the same dish were examined at once. The mean of these determinations was used to estimate H_2O_2 concentration for each sample.

Neutralizing Ab and metabolic inhibitor assays

Human lung fibroblasts were grown to confluence and rendered quiescent in SFDM for 24 h. Cells were pretreated for 1 h with each of the following Abs at a concentration of 0.1 μg/ml: neutralizing anti-IFN-α, neutralizing anti-IFN-β, or IgG (R&D Systems). Other dishes of cells were pretreated for 1 h with one of the following metabolic inhibitors: 15 μM DPI, 100 μM apocynin or allopurinol, 4 μM JAK I inhibitor InSolution, or 1000 U/ml catalase. Cells were subsequently exposed to V_2O_5 (10 μg/cm^2) in the presence of Ab or inhibitor. Supernatants were aspirated and cell lysates processed for RNA or Western blot analysis as described below.

Preparation of cellular protein and RNA

Human lung fibroblasts were grown to confluence in 60-mm dishes and rendered quiescent in SFDM for a minimum of 24 h. Cell lysates were collected by washing the cells once with PBS on ice, scraping in 200 μl of PBS and centrifuging for 5 min at 10,000 $\times$ g. Supernatants were aspirated and cell lysates were processed for either protein or RNA. For protein, 125 μl of lysis buffer (50 mM Tris-HCl (pH 7.4), 1% Triton X-100, 150 mM NaCl, 1 mM EGTA, 1 mM PMSF, 0.25% sodium deoxycholate, 1 μg/ml aprotinin, 1 μg/ml leupeptin, 1 μg/ml pepstatin, 1 mM sodium vanadate, and 1 mM sodium fluoride) was added to the cells. The lysed cells were sonicated for 5 min and spun in a microfuge at maximum speed for 5 min to fractionate insoluble DNA and chromatin proteins from soluble cellular proteins. Total RNA was isolated using the Qiagen RNeasy Miniprep kit according to the manufacturer's instructions (Qiagen).

Western blot analysis

Samples were separated by SDS-PAGE, transferred to nitrocellulose membranes, and blocked for 1 h in 5% nonfat milk in TBS (20 mM Tris, 137 mM NaCl and 0.1% Tween 20). The blot was then incubated at 4°C overnight in a 1/1000 dilution of primary Ab followed by incubation for 1 h in a 1/2000 dilution of HRP- or alkaline phosphatase-conjugated secondary Ab. The immunoblot signal was detected and visualized through ECL or enhanced chemifluorescence (Amersham Biosciences). For reprobing, the blot was stripped of Ab and signal by incubating the membrane in stripping buffer (62.5 mM Tris (pH 6.7), 2% SDS, 100 mM 2-ME) for 30 min at 50°C.

TaqMan real-time quantitative RT-PCR

Total RNA from human lung fibroblasts was isolated using the Qiagen RNeasy Miniprep kit. One microgram of total RNA was reverse-transcribed at 48°C for 30 min using Multiscribe Reverse Transcriptase (RT; Applied Biosystems) in 1$\times$ RT buffer, 5.5 mM $MgCl_2$, 0.5 μM of each dNTP, 2.5 μM of random hexamers, and 0.4 U/μl RNase inhibitor in a volume of 100 μl. Fifty nanograms of the RT product were amplified using TaqMan Gene Expression Assays specific for IFN-α, IFN-β, or CXCL10 and analyzed on the Applied Biosystems 7700 Prism Sequence Detection System. The PCR conditions and data analysis were performed according to the manufacturer's protocol (user bulletin no. 2; Applied Biosystems Prism 7700 Sequence Detection System). All samples were run in triplicate. Gene expression was measured by the quantitation of cDNA converted from mRNA corresponding to gene of interest relative to the untreated control groups and normalized to 18S ribosomal RNA. Relative quantitation values ($2^{-\Delta\Delta CT}$, where CT is the cycle threshold) were expressed as fold-change.

CXCL10 ELISA

CXCL10 protein in fibroblast-conditioned medium was measured using a commercially available ELISA (R&D Systems).

Cell proliferation and collagen assays

Fibroblast proliferation was measured using a colorimetric BrdU ELISA kit (cat. no. 11647229001) according to the manufacturer's instructions (Roche Diagnostics). Positive control for proliferation was 10% FBS and negative control was SFDM. Collagen protein levels were measured using the Sircol assay according to the manufacturer's instructions (Biocolor Life Science; www.biocolor.co.uk). As a positive control, cells were treated with 10 ng/ml rTGF-β1 (R&D Systems) or treated with SFDM as a negative control.

Statistics

All data were plotted and analyzed using the GraphPad Prism software. A one-way ANOVA was used to test for differences between treatment groups with post-hoc comparisons by Tukey's multiple comparison test. A two-way ANOVA with a post-hoc Bonferroni test was used for multiple treatments over a time course. A value of $p < 0.05$ was considered significant.

Results

V_2O_5-induced STAT-1 activation in human lung fibroblasts is blocked by a NADPH oxidase inhibitor

V_2O_5-induced STAT-1 activation was observed in lung fibroblasts from three different donors (ATCC lines 16Lu, 19Lu, and 11Lu). V_2O_5-induced STAT-1 phosphorylation in the absence or presence of DPI was measured by Western blot analysis using Abs against phosphorylated (Tyr^{701}) STAT-1 or total STAT-1 protein (Fig. 1*A*). Densitometric analysis of the ratio of pSTAT-1/STAT-1 was

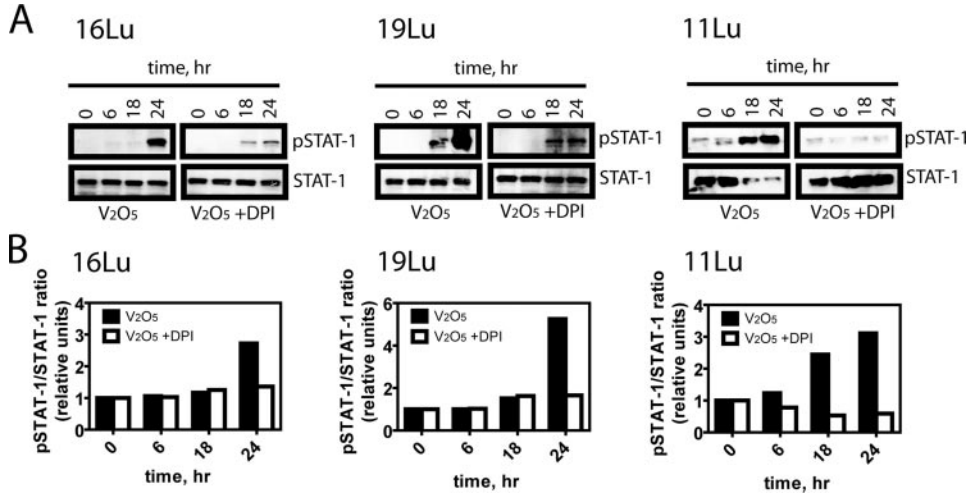

FIGURE 1. V_2O_5-induced STAT-1 phosphorylation in cultured human lung fibroblasts is blocked by DPI, a broad spectrum NADPH oxidase inhibitor. Normal diploid human lung fibroblasts from three different donors (16Lu, 19Lu, 11Lu) were grown to confluency in 10% FBS-DMEM and then rendered quiescent in SFDM for 24 h. Cells were treated with DPI (15 μM) delivered in DMSO vehicle or DMSO alone as a control for 1 h, then treated with V_2O_5 (10 μg/cm^2); cell lysates were collected at various time points as described in *Materials and Methods*. *A*, Representative Western blots of phosphorylated STAT-1 (pSTAT-1) and total STAT-1 protein in 16Lu, 19Lu, and 11Lu human lung fibroblasts. *B*, Densitometry of the blots in *A* showing the relative ratio of pSTAT-1 to total STAT-1 in each cell line.

performed to quantify the inhibition of STAT-1 phosphorylation in the presence of DPI (Fig. 1*B*). V_2O_5 exposure activated STAT-1 in cultured human lung fibroblasts in a delayed manner at 18–24 h (Fig. 1) as compared with IFN-induced STAT-1 phosphorylation observed within 15–30 min (data not shown). V_2O_5-induced STAT-1 phosphorylation was completely inhibited by DPI, a flavoprotein inhibitor that blocks NADPH oxidase-mediated H_2O_2 generation. The temporal pattern of V_2O_5-induced STAT-1 activation and sensitivity to DPI was consistent in all three human lung fibroblast lines tested.

V_2O_5 stimulates the production of intracellular reactive oxygen species (ROS) and the release of H_2O_2 into fibroblast-conditioned medium

To determine whether V_2O_5 increased intracellular H_2O_2, we loaded fibroblasts with CM-H_2DCFDA, a cell-permeable dye that is converted to an insoluble fluorescent product in the presence of H_2O_2. V_2O_5 significantly increased intracellular H_2O_2 in a time-dependent manner that peaked at 18 h post-exposure (Fig. 2*A*). Furthermore, we measured extracellular H_2O_2 levels in fibroblast conditioned medium using the Amplex Red assay and showed a similar peak in H_2O_2 released from cells at 18 h post-V_2O_5 treatment (Fig. 2*B*).

V_2O_5 stimulates IFN-α and IFN-β mRNA transcription that is blocked by DPI

Our previous work demonstrated that V_2O_5-induced STAT-1 activation was inhibited by cycloheximide, indicating a requirement for de novo protein synthesis (11). IFNs are well-known activators of STAT-1 (6, 7). Therefore, we analyzed V_2O_5-treated cells for IFN mRNA levels by TaqMan quantitative real-time RT-PCR. IFN-α mRNA levels were increased 10-fold at 6 h, but maximal

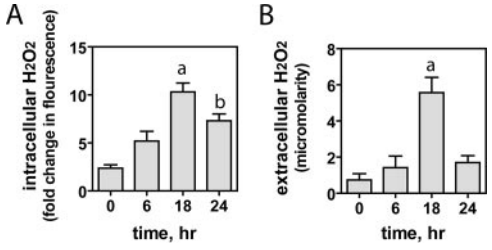

FIGURE 2. V_2O_5 exposure increases H_2O_2 levels in cultured human lung fibroblasts. Confluent 16Lu human lung fibroblasts were serum starved for 24 h and then treated with V_2O_5 (10 μg/cm^2) for the indicated time points. *A*, Intracellular H_2O_2 levels were measured using the fluorescent dye CM-H_2DCFDA. Cells were incubated with 10 μM CM-H_2DCFDA for 30 min. Equal numbers of cells were loaded on a fluorescence plate reader and fluorescence was measured at excitation wavelength 485 nm and emission wavelength 538 nm. After background correction, fluorescence was expressed as a fold change over time-matched untreated cells. Data are the mean ± SEM of three experiments each repeated in triplicate. *a*, ***, $p < 0.001$ compared with zero time point; *b*, *, $p < 0.05$ compared with zero time point. *B*, Extracellular H_2O_2 was measured using the Amplex Red assay. Quiescent fibroblasts were treated with V_2O_5 (10 μg/cm^2) and conditioned medium collected at the indicated time points. Data are the mean ± SEM of three experiments each repeated in duplicate. *a*, **, $p < 0.01$ compared with zero time point.

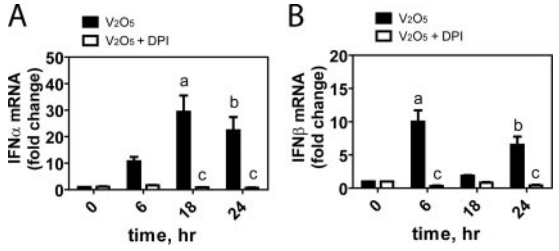

FIGURE 3. V_2O_5-induced IFN-α and IFN-β mRNA transcription is inhibited by DPI. 16Lu human lung fibroblasts were grown to confluency, serum starved for 24 h, pretreated for 1 h with either vehicle control DMSO (■) or DPI (15 μM) (□) and subsequently exposed to 10 μg/cm^2 V_2O_5. mRNA isolated at indicated times was analyzed by TaqMan real-time quantitative RT-PCR. IFN mRNA levels were normalized to 18S ribosomal RNA and expressed as fold change relative to untreated time-matched controls. Data are presented as mean values ± SD from triplicate samples and are representative of three independent experiments with similar results. *A*, IFN-α results showing induction by V_2O_5: (*a*) **, $p < 0.01$ or (*b*) *, $p < 0.05$ compared with zero time point, and inhibition by DPI: (*c*) ***, $p < 0.001$ compared with V_2O_5 time-matched treatment. *B*, IFN-β results showing induction by V_2O_5: (*a*) **, $p < 0.01$ or (*b*) *, $p < 0.05$ compared with zero time point, and inhibition by DPI: (*c*) ***, $p < 0.001$ compared with V_2O_5 time-matched treatment.

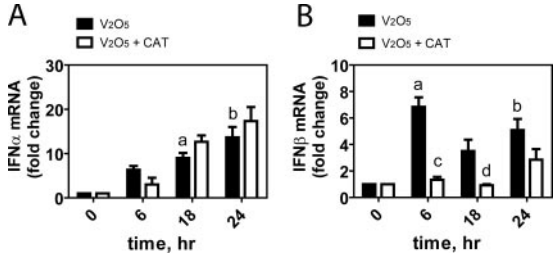

FIGURE 4. V_2O_5-induced transcription of IFN-β but not IFN-α is inhibited by catalase, a selective scavenger of H_2O_2. 16Lu human lung fibroblasts were grown to confluency, serum starved for 24 h, pretreated for 1 h with either vehicle control DMSO (■) or catalase (1000 U/ml) (□) and subsequently exposed to 10 μg/cm^2 V_2O_5. mRNA isolated at indicated times was analyzed by TaqMan real-time quantitative RT-PCR. IFN mRNA levels were normalized to 18S ribosomal RNA and expressed as fold change relative to untreated time-matched controls. Data are presented as mean values ± SD from triplicate samples and are representative of three independent experiments with similar results. *A*, IFN-α results showing induction by V_2O_5: (*a*) *, $p < 0.05$ or (*b*) ***, $p < 0.001$ compared with zero time point. DPI did not significantly affect IFN-α mRNA levels. *B*, IFN-β results showing induction by V_2O_5: (*a*) **, $p < 0.01$ or (*b*) *, $p < 0.05$ compared with zero time point, and inhibition by DPI: (*c*) ***, $p < 0.001$ or (*d*) *, $p < 0.05$ compared with V_2O_5 time-matched treatment.

induction (20- to 30-fold) occurred between 18 and 24 h (Fig. 3*A*). IFN-β mRNA levels were increased 5- to 10-fold at 6 h posttreatment, and a second peak of induction in IFN-β was observed at 24 h (Fig. 3*B*). IFN-γ mRNA was not detected in human lung fibroblasts (data not shown). V_2O_5-induced IFN-α and IFN-β transcription was significantly blocked by DPI (Fig. 3).

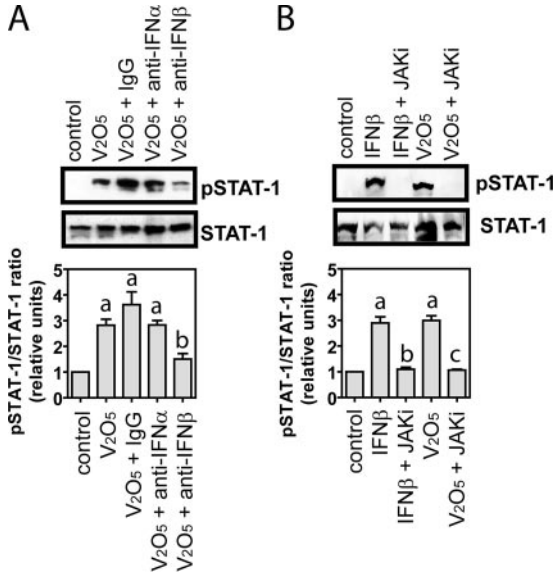

FIGURE 5. IFN-β and Jak kinases are required for STAT-1 phosphorylation by V_2O_5. 16Lu human lung fibroblasts were cultured either in the absence or presence of 0.1 μg/ml polyclonal neutralizing Abs to IFN-α and IFN-β (*A*) or 4 μM Jak I InSolution inhibitor (*B*) for 1 h before the addition of 10 μg/cm^2 V_2O_5 for 24 h or 1000 U/ml IFN-β for 30 min. Western blot analysis was performed on cell lysates to determine pSTAT-1 and total STAT-1 levels. Representative Western blots are shown. Densitometry was performed on three separate experiments to show the relative ratio of pSTAT-1 to total STAT-1. Data are the mean ± SEM. *A*, Significant phosphorylation of STAT-1 by V_2O_5 alone or by V_2O_5 in the presence of IgG or anti-IFN-α (*a*, **, $p < 0.01$), and significant reduction in V_2O_5-induced STAT-1 phosphorylation by anti-IFN-β (*b*, *, $p < 0.05$) compared with V_2O_5. *B*, Significant phosphorylation of STAT-1 by V_2O_5 or IFN-β (*a*, ***, $p < 0.001$) compared with control and significant reduction in STAT-1 phosphorylation by JAK inhibitor (*b*, ***, $p < 0.001$) compared with IFN-β, or (*c*, ***, $p < 0.001$) compared with V_2O_5.

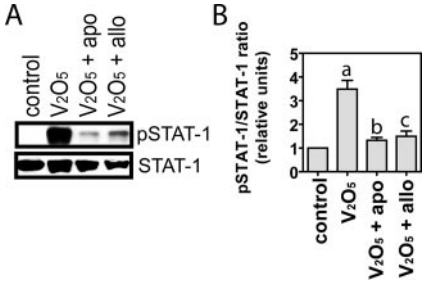

FIGURE 6. Phosphorylation of STAT-1 is blocked by an NADPH oxidase inhibitor (apocynin) and a xanthine oxidase inhibitor (allopurinol). 16Lu human lung fibroblasts were grown to confluency, rendered quiescent, and pretreated for 1 h with vehicle control DMSO, NADPH oxidase inhibitor apocynin (100 μM), or xanthine oxidase inhibitor allopurinol (100 μM). Cells were then treated with V_2O_5 (10 μg/cm^2) and cell lysates were harvested for Western blotting. *A*, Representative Western blot analysis of phosphorylated STAT-1 (pSTAT-1) and total STAT-1. *B*, Densitometry was performed on three independent experiments to determine the relative ratio of pSTAT-1 to total STAT-1. Data are the mean ± SEM. V_2O_5 caused a significant phosphorylation of STAT-1 (*a*, ***, $p < 0.001$) compared with control. STAT-1 phosphorylation was blocked by apocynin (*b*, ***, $p < 0.001$) or allopurinol (*c*, **, $p < 0.01$) compared with V_2O_5.

Differential effect of catalase on V_2O_5-induced IFN-α and IFN-β mRNA levels

Although DPI is a broad spectrum NADPH oxidase inhibitor, catalase is a selective scavenger of H_2O_2. Because H_2O_2 is generated by V_2O_5 exposure in human lung fibroblasts (Fig. 2), we postulated that IFN mRNA levels increased by V_2O_5 were mediated by elevated H_2O_2. V_2O_5-induced IFN-α mRNA levels were not reduced significantly by catalase (Fig. 4*A*). In contrast, catalase significantly inhibited V_2O_5-induced IFN-β mRNA levels at 6 and 18 h (Fig. 4*B*).

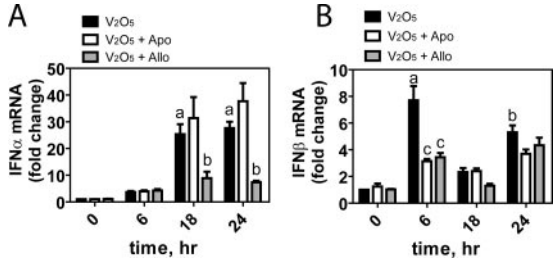

FIGURE 7. IFN-α and IFN-β transcription are differentially regulated by NADPH oxidase and xanthine oxidase. Confluent cultures of 16Lu human lung fibroblasts were rendered quiescent and either pretreated for 1 h with vehicle control DMSO (■), or NADPH oxidase inhibitor apocynin (100 μM) (□) or xanthine oxidase inhibitor allopurinol (100 μM) (▨) and subsequently treated with V_2O_5 (10 μg/cm^2). Samples were analyzed for IFN mRNA levels by TaqMan quantitative real-time RT-PCR. Samples were normalized to 18S ribosomal RNA and expressed as fold change relative to untreated time-matched controls. Data are presented as mean values ± SD from triplicate samples and are representative of three independent experiments with similar results. *A*, IFN-α results showing induction by V_2O_5 (*a*, ***, $p < 0.001$) compared with zero time point, and inhibition by allopurinol (*b*, **, $p < 0.01$) compared with V_2O_5 time-matched treatment. *B*, IFN-β results showing induction by V_2O_5 (*a*, ***, $p < 0.001$ or *b*, **, $p < 0.01$) compared with zero time point, and inhibition by apocynin or allopurinol at 6 h posttreatment (*c*, ***, $p < 0.001$) compared with V_2O_5 time-matched treatment.

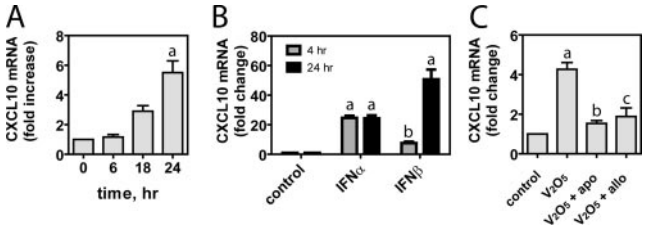

FIGURE 8. CXCL10 mRNA is up-regulated by vanadium and type I IFNs and is H_2O_2 dependent. 16Lu human lung fibroblasts were grown to confluency, rendered quiescent for 24 h, and subsequently exposed to 10 μg/cm^2 V_2O_5 (*A*), 1000 U/ml IFN-α or IFN-β (*B*), or treated with V_2O_5 in the presence of NADPH oxidase inhibitor apocynin (100 μM) or xanthine oxidase inhibitor allopurinol (100 μM) (*C*). RNA was isolated at indicated times and analyzed by TaqMan real-time quantitative RT-PCR. CXCL10 mRNA levels were normalized to 18S ribosomal RNA and expressed as fold change relative to untreated controls. Data are presented as mean values ± SD from triplicate samples and are representative of three independent experiments with similar results. *A*, V_2O_5 significantly increases CXCL10 mRNA levels (*a*, ***, $p < 0.001$) compared with time zero. *B*, Both IFNs increase CXCL10 (*a*, ***, $p < 0.001$ or *b*, *, $p < 0.05$) compared with control. *C*, Either apocynin or allopurinol inhibits V_2O_5-induced CXCL10 mRNA levels (*b*, ***, $p < 0.001$ or *c*, **, $p < 0.01$) compared with V_2O_5.

V_2O_5 induced STAT-1 phosphorylation is IFN dependent

The Jak1 and Tyk2 kinases are associated with the type I IFN receptor and are responsible for transducing signals from the receptor to STAT-1 (18, 19). To further confirm that V_2O_5-induced STAT-1 phosphorylation was type I IFN dependent, fibroblasts were incubated in the presence of polyclonal control Ab, neutralizing Abs to IFN-α or IFN-β, or a pan-specific inhibitor for JAK (InSolution Jak inhibitor I) during V_2O_5 exposure. Fibroblasts were also treated with IFN-β (as a positive control) and cell lysates were analyzed for phosphorylated and total STAT-1 by Western analysis. V_2O_5-induced STAT-1 phosphorylation was not significantly decreased by neutralizing anti-IFN-α Ab while a neutralizing anti-IFN-β Ab significantly reduced V_2O_5-induced STAT-1 phosphorylation (Fig. 5*A*). In addition, V_2O_5-induced STAT-1 phosphorylation was completely blocked by JAK inhibitor InSolution I (Fig. 5*B*).

Phosphorylation of STAT-1 is dependent on both NADPH oxidase and xanthine oxidase

Because DPI is a broad spectrum flavoprotein inhibitor, it inhibits other flavoproteins such as xanthine oxidase in addition to NADPH oxidase. To ascertain the relative contribution of NADPH oxidase and xanthine oxidase as enzymatic sources of H_2O_2 that mediated STAT-1 phosphorylation, fibroblasts were pretreated with apocynin (NADPH oxidase inhibitor) (20) or allopurinol (xanthine oxidase inhibitor) (21). Apocynin or allopurinol markedly reduced V_2O_5-induced STAT-1 phosphorylation at 24 h post-exposure (Fig. 6).

V_2O_5-induced IFN-α and IFN-β mRNA levels are differentially regulated by NADPH oxidase and xanthine oxidase

Because both apocynin and allopurinol blocked the phosphorylation of STAT-1, experiments were conducted to determine whether these inhibitors influence type I IFN mRNA levels. The xanthine oxidase inhibitor allopurinol significantly decreased V_2O_5-induced IFN-α mRNA levels throughout the time period analyzed (Fig. 7*A*) and inhibited early induction of IFN-β mRNA at 6 h (Fig. 7*B*). The NADPH oxidase inhibitor apocynin inhibited V_2O_5-induced IFN-β mRNA at 6 h (Fig. 7*B*), but did not decrease V_2O_5-induced IFN-α mRNA levels (Fig. 7*A*). These data indicate that inhibition of STAT-1 protein phosphorylation by apocynin and allopurinol (Fig. 6) is mediated via reduction of *IFN-β* gene transcription, because apocynin had no affect on IFN-α transcription (Fig. 7*A*).

V_2O_5 induction of IFN-inducible chemokine CXCL10 is mediated by NADPH and xanthine oxidases

Our recent Affymetrix microarray analysis of V_2O_5-treated human lung fibroblasts revealed induction of a STAT-dependent chemokine, CXCL10 (17). Quantitative real-time RT-PCR confirmed that V_2O_5 increased gene expression of CXCL10 occurred with a temporal expression pattern similar to that of STAT-1 phosphorylation (Fig. 8*A*). We further demonstrated that IFN-α and IFN-β up-regulate CXCL10 expression in fibroblasts as early as 4-h post-exposure, and yet only IFN-β caused a strong, sustained induction of CXCL10 up to 24 h (Fig. 8*B*). V_2O_5-induced CXCL10 mRNA levels were inhibited by both apocynin and allopurinol (Fig. 8*C*), indicating that both xanthine oxidase and NADPH oxidase are required for V_2O_5-induced CXCL10 gene expression. Although both IFN-α and IFN-β increase CXCL10 mRNA levels, V_2O_5-induced IFN-β and CXCL10 mRNA levels are blocked by apocynin and allopurinol. In contrast, V_2O_5-induced IFN-α was blocked only by allopurinol while apocynin had no inhibitory effect. These results suggest that V_2O_5 induction of CXCL10 is mediated by IFN-β and is dependent on both NADPH oxidase and xanthine oxidase.

V_2O_5-induced CXCL10 protein secretion is blocked by pretreatment with DPI and reproducible in several different human lung fibroblasts isolates

CXCL10 protein secreted into the fibroblast-conditioned medium was increased by V_2O_5 in 16Lu, 19Lu and, 11Lu human lung

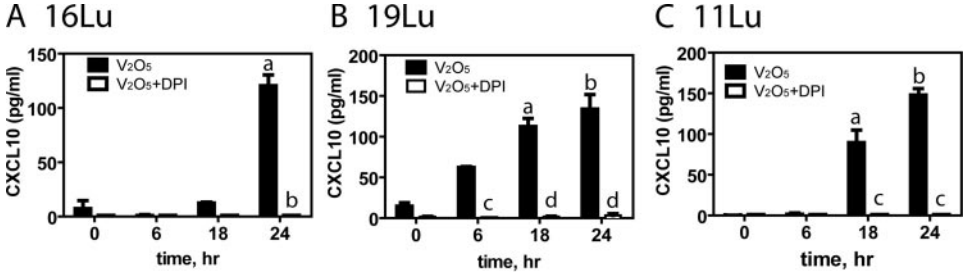

FIGURE 9. V_2O_5-induced secretion of CXCL10 protein from human lung fibroblasts is dependent on NADPH oxidase activity. Human lung fibroblasts from three different donors (16Lu, 19Lu, and 11Lu) were grown to confluency in 10% FBS-DMEM and the rendered quiescent in SFDM for 24 h. Cells were treated with DPI (15 μM) delivered in DMSO or DMSO alone as a control for 1 h, then treated with V_2O_5 (10 μg/cm^2); conditioned medium was harvested at the indicated time points. CXCL10 protein secreted into the condition medium was measured by ELISA. Data are from a single experiment performed in duplicate for each cell line. *A*, Results with 16Lu fibroblasts: (*a*) ***, $p < 0.001$ compared with zero time point and (*b*) ***, $p < 0.001$, compared with V_2O_5. *B*, 19Lu fibroblasts: (*a*) **, $p < 0.01$ or (*b*) ***, $p < 0.001$ compared with time zero, and (*c*) **, $p < 0.01$ or (*d*) ***, $p < 0.001$ compared with time-matched V_2O_5 treatment. *C*, 11Lu fibroblasts (*a*) *, $p < 0.05$ or (*b*) **, $p < 0.01$ compared with zero time point, and (*c*) ***, $p < 0.001$ compared with time-matched V_2O_5 treatment.

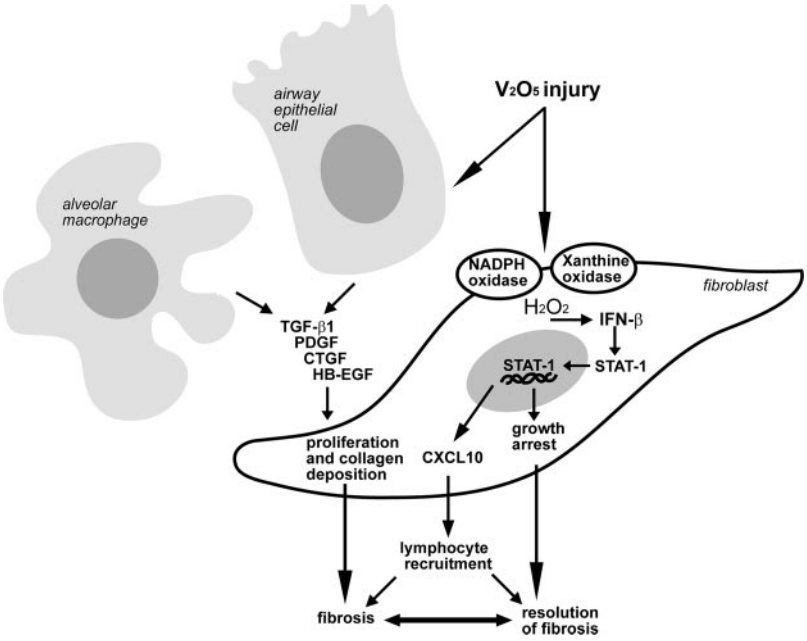

FIGURE 10. Postulated mechanism of V_2O_5-induced STAT-1 signaling mediated by IFN-β in human lung fibroblasts. First, vanadium activates cell surface NADPH oxidase and cytoplasmic xanthine oxidase. Next, H_2O_2 generated by these oxidases increase IFN-β transcription. The autocrine release of IFN-β by fibroblasts stimulates STAT-1 phosphorylation. Activated STAT-1 then translocates to the nucleus and binds specific promoter regions that regulate growth arrest and induction of CXCL10 chemokine expression. Lymphocytes recruited by CXCL10 could play a role in fibrosis or the resolution of fibrosis. The antifibrotic activities of IFN, STAT-1, and CXCL10 are proposed to counteract profibrotic growth factors signals such as CTGF, HB-EGF, PDGF, and TGF-β1 from macrophages and epithelial cells.

fibroblasts (Fig. 9). Additionally, pretreatment with DPI for 1 h completely inhibited V_2O_5-induced secretion of CXCL10 in all three fibroblast lines. These findings closely mirror the results obtained for STAT-1 phosphorylation induced by V_2O_5 for these fibroblast lines (Fig. 1).

V_2O_5 does not directly stimulate fibroblast proliferation or collagen production in human lung fibroblasts

Although V_2O_5 causes fibrosis, it remains unclear whether V_2O_5 stimulates proliferation and collagen production in fibroblasts directly or whether other cell types orchestrate the proliferative and matrix deposition responses of fibroblasts via paracrine signals. V_2O_5 (10 μg/cm^2) did not cause a significant change in human lung fibroblast (16Lu) proliferation as measured by BrdU ELISA over a 24-h time course (data not shown). Moreover, V_2O_5 did not increase TGF-β1 mRNA levels in 16Lu fibroblasts as measured by TaqMan quantitative RT-PCR and actually decreased procollagen mRNA levels by ~70% at 24-h post-V_2O_5 treatment. However, collagen protein levels measured by Sircol assay were only marginally decreased (~10%) at 24 h post-V_2O_5 treatment (data not shown). These data suggest that V_2O_5 does not directly cause an increase in fibroblast proliferation or collagen deposition, but instead that V_2O_5 likely stimulates other pulmonary cell types to release factors that drive these fibrogenic endpoints in vivo.

Discussion

The regulation of fibroblast growth is a key determinant in the progression or resolution of fibrosis. STAT-1 is an important regulator of fibroblast growth arrest. We previously reported that V_2O_5-induced STAT-1 phosphorylation requires hours to occur and is blocked by cycloheximide indicating de novo protein synthesis and production of an autocrine mediator (11). In the present study, we sought to identify the de novo protein(s) that mediated V_2O_5-induced STAT-1 activation in human lung fibroblasts. We report for the first time that V_2O_5 increases the production of type I IFNs (IFN-α and IFN-β), which are potent STAT-1 activators. Furthermore, we identified that IFN-β as the primary mediator of V_2O_5-induced STAT-1 phosphorylation and identified CXCL10 as a downstream target gene of IFN-β. A hypothetical mechanism through which V_2O_5 activates STAT-1 via IFN-β in lung fibroblasts is illustrated in Fig. 10.

IFNs mediate many of their biological actions through STAT-1, including the suppression of growth factor-induced proliferation of fibroblasts (7, 8, 10). V_2O_5-induced STAT-1 activation was decreased in the presence of neutralizing Abs to IFN-β, but not IFN-α. We also demonstrated that V_2O_5-induced type I IFN mRNA expression and STAT-1 activation were NADPH oxidase and xanthine oxidase dependent. The requirement of JAK for STAT-1 activation by IFNs has been previously established (18, 19). V_2O_5-induced STAT-1 phosphorylation was abolished by the JAK inhibitor, which supports our hypothesis that STAT-1 activation is dependent on autocrine IFN production and signaling through the IFN receptor.

IFN-α and IFN-β mRNAs exhibited markedly different temporal expression patterns in response to V_2O_5 treatment, suggesting that different mechanisms regulate the production of these two IFNs in response to metal-induced oxidative stress. IFN-β mRNA expression peaked at 6 h and preceded the induction of IFN-α transcription at 18–24 h post V_2O_5 exposure. IFN-β stimulates the JAK-STAT pathway through the IFN receptor, resulting in activation of the transcription factor IFN-stimulated gene factor 3 (*ISGF3*) that in turn increases IFN regulatory factor 7 protein synthesis (22). IFN regulatory factor 7 has been shown to amplify IFN-α expression through a positive feedback loop (23). This suggests that early induction of IFN-β by V_2O_5 in our experiments could stimulate an increase in IFN-α at later time points.

Because IFN-α mRNA and phosphorylation of STAT-1 temporally coincide, we initially presumed that IFN-α was the more likely candidate that stimulated STAT-1 phosphorylation. However, both apocynin and allopurinol blocked phosphorylation of STAT-1, while IFN-α transcription was not affected by apocynin. In addition, we also demonstrated that preincubation with neutralizing IFN-β Ab but not neutralizing IFN-α blocked phosphorylation of STAT-1. These data indicate that IFN-β levels govern V_2O_5-induced STAT-1 phosphorylation.

The mechanism through which V_2O_5-induced oxidative stress mediates type I IFN production is not known. However, it appears that H_2O_2 plays a key role in IFN induction by V_2O_5. We used an

H_2O_2-sensitive, cell-permeable fluorescent probe, DCFDA, to measure intracellular levels of H_2O_2 in response to V_2O_5. Increased levels were observable as early as 1-h post-treatment and peaked at 18 h. Extracellular levels of H_2O_2 generated in response to V_2O_5 were also monitored by an Amplex Red assay with a cell-impermeable, fluorescent dye with maximum levels also observed at 18 h. There are limitations to both of these assays. DCFDA can react with ROS other than H_2O_2 as well as heme proteins or redox-active metal ions (24), resulting in overestimation of intracellular H_2O_2 levels. In the Amplex Red assay, endogenous catalase can compete with HRP, leading to underestimation of extracellular H_2O_2 (24). However, the data from these two different endpoints (extracellular and intracellular H_2O_2) using fluorescent probes with different modes of activation (directly by H_2O_2 or indirectly by catalase) are in agreement, and together argue strongly in support of significant cellular H_2O_2 production in response to V_2O_5.

It is possible that ROS generated by V_2O_5 other than H_2O_2 could mediate increased IFN-β production. For example, ·OH is known to activate NF-κB, and this ROS-mediated activation is blocked by the antioxidant *N*-acetyl-L-cysteine (25). In addition, we have observed that V_2O_5 activates NF-κB within 30 min in pulmonary fibroblasts (Y. Wang and J. C. Bonner, unpublished observation). NF-κB regulates the expression of numerous inflammatory mediators, including type I IFNs (6). Therefore, it is possible that activation of NF-κB by V_2O_5 could contribute to induction of type I IFNs and STAT-1 activation. However, this hypothesis remains to be tested in human lung fibroblasts.

Our initial experiments used DPI, a flavoprotein inhibitor that has broad selectivity for NADPH and xanthine oxidase systems. Additional experiments were conducted using the selective NADPH oxidase inhibitor apocynin and the xanthine oxidase inhibitor allopurinol. Allopurinol inhibited V_2O_5-induced phosphorylation of STAT-1 and also blocked V_2O_5-induced IFN-α and IFN-β mRNA expression. Apocynin also inhibited IFN-β mRNA expression by V_2O_5, but not IFN-α, mRNA levels. These data suggest that both NADPH and xanthine oxidase activity drive IFN-β transcription. Moreover, we speculate that because the IFN-α mRNA level is significantly reduced by allopurinol, ROS generated via the xanthine oxidase system drives IFN-α transcription 18–24 h post-V_2O_5 exposure. We also used catalase to reduce cell-derived H_2O_2 generated by V_2O_5 exposure. Exogenously added catalase does not likely enter the intracellular compartment. However, H_2O_2 is freely diffusible across the cell membrane and the rapid depletion or scavenging of extracellular H_2O_2 with catalase in turn reduces the intracellular redox status (26). Catalase did not significantly reduce levels of IFN-α mRNA post-V_2O_5 treatment, but did significantly block IFN-β mRNA levels post-V_2O_5 treatment. Therefore, while H_2O_2 may be important in regulating IFN-β levels, it is possible that ROS other than H_2O_2 are important in regulating V_2O_5-induced IFN-α.

In a previous report on global gene analysis of human lung fibroblasts exposed to V_2O_5 in vitro, we observed that CXCL10, an IFN-inducible STAT-1-dependent gene, was increased in a time-dependent manner (17). In the present study, we confirmed this observation using quantitative real-time RT-PCR and ELISA. In addition, we showed that IFN-α and IFN-β induced CXCL10 in human lung fibroblasts, which is similar to the findings of others using different cell types (27, 28). Furthermore, apocynin or allopurinol inhibited *CXCL10* gene expression and this closely correlated with inhibition of IFN-β mRNA transcription in the presence of these two inhibitors. Thus, our data indicate that V_2O_5 increases CXCL10 through IFN-β and this pathway is dependent on NADPH and xanthine oxidase activity.

CXCL10 is a pleiotropic molecule that elicits potent biological effects including chemotaxis of activated T and NK cells, modulation of adhesion molecule expression, and inhibition of angiogenesis (29, 30). CXCL10 reduces bleomycin-induced pulmonary fibrosis in mice via inhibition of angiogenesis (31). Deletion of CXCR3, the receptor for CXCL10, increases bleomycin-induced fibroproliferation and mortality in mice (32). IFNs reduce fibroblast proliferation through transcriptionally active STAT-1 and increase CXCL10 production (33). Alternatively, CXCL10 induces the production of IFN-γ by lymphocytes in vivo in the lungs of mice (31). We have previously reported that STAT-1-deficient mice are susceptible to pulmonary fibrosis and this was correlated with a lack of growth inhibition in the presence of IFN-γ in fibroblasts isolated from the lungs of STAT-1 null mice (10). Therefore, our findings support the hypothesis that STAT-1, IFNs, and CXCL10 are protective factors in the lung that limit the severity of a fibrogenic response and promote the resolution of fibrosis.

The primary focus of this investigation was to elucidate a mechanism that mediates the resolution of fibrosis after V_2O_5 injury. How then does V_2O_5 cause fibrosis and what determines balance between fibrosis and resolution after injury? Our past studies have shown that V_2O_5 causes airway fibrosis in the lungs of rats and mice after a single intratracheal exposure (3, 34). Others have reported that V_2O_5 causes occupational bronchitis in humans (1, 2). In the present study, we found that V_2O_5 did not stimulate fibroblast proliferation in vitro, nor did it increase collagen synthesis or increase TGF-β1, the key growth factor that stimulates collagen synthesis. These findings are consistent with recent work from our laboratory wherein we showed that collagen genes (*COL1A2*, *COL1A1*, *COL3A1*), along with TGF-β2 and its associated signaling intermediates SMAD1 and SMURF1 were all down-regulated by V_2O_5 in cultures of 16Lu human lung fibroblasts (17). However, V_2O_5 increases TGF-β1 and collagen in the lungs of mice and rats. Most recently, we found that TGF-β1 protein in the bronchoalveolar lavage fluid of mice exposed to V_2O_5 is highly induced (40 pg/ml) as compared with saline control groups where no TGF-β1 was detected (J. P. Ryman-Rasmussen and J. C. Bonner, unpublished observation). During pulmonary fibrosis, the majority of TGF-β1 in the lungs are produced by activated alveolar macrophages and epithelial cells (35). The airway epithelium and lung macrophages also produce other growth factors that are likely important to fibroblast proliferation and collagen deposition. We have observed that connective tissue growth factor (CTGF) mRNA is increased several-fold for up to 24 h in cultured human lung epithelial cells (H292; ATCC) exposed to V_2O_5 and CTGF mRNA is increased several fold in whole lung tissue after 21 days in mice exposed to V_2O_5 by intratracheal aspiration (E. A. Turpin and J. C. Bonner, unpublished observations). We previously reported that V_2O_5 stimulates human bronchial epithelial cells to release heparin-binding EGF (HB-EGF), a potent mitogen for human lung fibroblasts (16). Finally, epithelial cells and macrophages are a rich source of PDGF, a potent mitogen for fibroblasts (5, 9). Therefore, while V_2O_5 does not directly stimulate fibroblast growth and collagen deposition by fibroblasts, these cells are stimulated by soluble growth factors from other pulmonary cell types that promote fibroblast replication and collagen deposition leading to fibrosis.

In summary, we report a novel mechanism that extends our understanding of vanadium-induced activation of STAT-1 as IFN dependent and establishes a role for the H_2O_2-generating enzymes NADPH oxidase and xanthine oxidase in type I IFN production. As depicted in Fig. 10, the autocrine production of IFN-β stimulates synthesis of CXCL10 that further contributes to the innate

immune response to metal-induced oxidative stress. This mechanism was reproducible in three different normal human lung fibroblasts lines. We postulate that these IFN-β-dependent signaling events are important to the resolution of fibrosis after V_2O_5 injury and counterbalance profibrogenic paracrine growth factor signals from epithelial cells and macrophages that drive fibroblast proliferation and collagen deposition.

Acknowledgments

We thank Drs. Wenhong Cao, Russell Thomas, and David Dorman for helpful comments during the preparation of this manuscript.

Disclosures

The authors have no financial conflict of interest.

References

1. Levy, B. S., L. Hoffman, and S. Gottsegen. 1984. Boilermakers' bronchitis: respiratory tract irritation associated with vanadium pentoxide exposure during oil-to-coal conversion of a power plant. *J. Occup. Med.* 26: 567–570.
2. Woodin, M. A., Y. Liu, D. Neuberg, R. Hauser, T. J. Smith, and D. C. Christiani. 2000. Acute respiratory symptoms in workers exposed to vanadium-rich fuel-oil ash. *Am. J. Ind. Med.* 37: 353–363.
3. Bonner, J. C., A. B. Rice, C. R. Moomaw, and D. L. Morgan. 2000. Airway fibrosis in rats induced by vanadium pentoxide. *Am. J. Physiol.* 278: L209–L216.
4. Razzaque, M. S., and T. Taguchi. 2003. Pulmonary fibrosis: cellular and molecular events. *Pathol. Int.* 53: 133–145.
5. Bonner, J. C. 2004. Regulation of PDGF and its receptors in fibrotic diseases. *Cytokine Growth Factor Rev.* 15: 255–273.
6. Stephanou, A., and D. S. Latchman. 2003. STAT-1: a novel regulator of apoptosis. *Int. J. Exp. Pathol.* 84: 239–244.
7. Malmgaard, L. 2004. Induction and regulation of IFNs during viral infections. *J. Interferon Cytokine Res.* 24: 439–454.
8. Stephanou, A., and D. S. Latchman. 2005. Opposing actions of STAT-1 and STAT-3. *Growth Factors* 23: 177–182.
9. Ingram, J. L., A. Antao-Menezes, J. B. Mangum, O. Lyght, P. J. Lee, J. A. Elias, and J. C. Bonner. 2006. Opposing actions of Stat1 and Stat6 on IL-13-induced up-regulation of early growth response-1 and platelet-derived growth factor ligands in pulmonary fibroblasts. *J. Immunol.* 177: 4141–4148.
10. Walters, D. M., A. Antao-Menezes, J. L. Ingram, A. B. Rice, A. Nyska, Y. Tani, S. R. Kleeberger, and J. C. Bonner. 2005. Susceptibility of signal transducer and activator of transcription-1-deficient mice to pulmonary fibrogenesis. *Am. J. Pathol.* 167: 1221–1229.
11. Wang, Y. Z., J. L. Ingram, D. M. Walters, A. B. Rice, J. H. Santos, B. Van Houten, and J. C. Bonner. 2003. Vanadium-induced STAT-1 activation in lung myofibroblasts requires H_2O_2 and P38 MAP kinase. *Free Radic. Biol. Med.* 35: 845–855.
12. Banfi, B., R. A. Clark, K. Steger, and K. H. Krause. 2003. Two novel proteins activate superoxide generation by the NADPH oxidase NOX1. *J. Biol. Chem.* 278: 3510–3513.
13. Lambeth, J. D. 2004. NOX enzymes and the biology of reactive oxygen. *Nat. Rev. Immunol.* 4: 181–189.
14. Harrison, R. 2002. Structure and function of xanthine oxidoreductase: where are we now? *Free Radic. Biol. Med.* 33: 774–797.
15. Ingram, J. L., A. B. Rice, J. Santos, B. Van Houten, and J. C. Bonner. 2003. Vanadium-induced HB-EGF expression in human lung fibroblasts is oxidant dependent and requires MAP kinases. *Am. J. Physiol.* 284: L774–L782.
16. Zhang, L., K. Adler, P. Sannes, L. Martin, W. Gladwell, J. Koo, T. E. Gray and J. C. Bonner. 2001. Vanadium stimulates human bronchial epithelial cells to produce HB-EGF: a mitogen for human lung fibroblasts. *Am. J. Respir. Cell Mol. Biol.* 24: 123–131.
17. Ingram, J. L., A. Antao-Menezes, E. A. Turpin, D. G. Wallace, J. B. Mangum, L. J. Pluta, R. S. Thomas, and J. C. Bonner. 2007. Genomic analysis of human lung fibroblasts exposed to vanadium pentoxide to identify candidate genes for occupational bronchitis. *Respir. Res.* 8: 34.
18. Muller, M., J. Briscoe, C. Laxton, D. Guschin, A. Ziemiecki, O. Silvennoinen, A. G. Harpur, G. Barbieri, B. A. Witthuhn, C. Schindler, et al. 1993. The protein tyrosine kinase JAK1 complements defects in interferon-α/β and -γ signal transduction. *Nature* 366: 129–135.
19. Velazquez, L., M. Fellous, G. R. Stark, and S. Pellegrini. 1992. A protein tyrosine kinase in the interferon α/β signaling pathway. *Cell* 70: 313–322.
20. Klees, R. F., P. C. De Marco, R. M. Salasznyk, D. Ahuja, M. Hogg, S. Antoniotti, L. Kamath, J. S. Dordick, and G. E. Plopper. 2006. Apocynin derivatives interrupt intracellular signaling resulting in decreased migration in breast cancer cells. *J. Biomed. Biotechnol.* 2006: 87246.
21. Pacher, P., A. Nivorozhkin, and C. Szabo. 2006. Therapeutic effects of xanthine oxidase inhibitors: renaissance half a century after the discovery of allopurinol. *Pharmacol. Rev.* 58: 87–114.
22. Genin, P., P. Morin, and A. Civas. 2003. Impairment of interferon-induced *IRF-7* gene expression due to inhibition of ISGF3 formation by trichostatin A. *J. Virol.* 77: 7113–7119.
23. Marie, I., J. E. Durbin, and D. E. Levy. 1998. Differential viral induction of distinct interferon-α genes by positive feedback through interferon regulatory factor-7. *EMBO J.* 17: 6660–6669.
24. Tarpey, M. M., D. A. Wink, and M. B. Grisham. 2003. Methods for detection of reactive metabolites of oxygen and nitrogen: in vitro and in vivo considerations. *Am. J. Physiol.* 286: R431–R444.
25. Chen, F., L. M. Demers, V. Vallyathan, M. Ding, Y. Lu, V. Castranova, and X. Shi. 1999. Vanadate induction of NF-κB involves IκB kinase β and SAPK/ERK kinase 1 in macrophages. *J. Biol. Chem.* 274: 20307–20312.
26. Preston, T. J., W. J. Muller, and G. Singh. 2001. Scavenging of extracellular H_2O_2 by catalase inhibits the proliferation of HER-2/Neu-transformed Rat-1 fibroblasts through the induction of a stress response. *J. Biol. Chem.* 276: 9558–9564.
27. Luster, A. D. 1998. Chemokines–chemotactic cytokines that mediate inflammation. *N. Engl. J. Med.* 338: 436–445.
28. Luster, A. D., and J. V. Ravetch. 1987. Biochemical characterization of a γ interferon-inducible cytokine (IP-10). *J. Exp. Med.* 166: 1084–1097.
29. Neville, L. F., G. Mathiak, and O. Bagasra. 1997. The immunobiology of interferon-γ inducible protein 10 kD (IP-10): a novel, pleiotrophic member of the C-X-C chemokine superfamily. *Cytokine Growth Factor Rev.* 8: 207–219.
30. Belperio, J. A., M. P. Keane, D. A. Arenberg, C. L. Addison, J. E. Ehlert, M. D. Burdick, and R. M. Strieter. 2000. CXC chemokines in angiogenesis. *J. Leukocyte Biol.* 68: 1–8.
31. Keane, M. P., J. A. Belperio, D. A. Arenberg, M. D. Burdick, Z. J. Xu, Y. Y. Xue, and R. M. Strieter. 1999. IFN-γ-inducible protein-10 attenuates bleomycin-induced pulmonary fibrosis via inhibition of angiogenesis. *J. Immunol.* 163: 5686–5692.
32. Jiang, D., J. Liang, J. Hodge, B. Lu, Z. Zhu, S. Yu, J. Fan, Y. Gao, Z. Yin, R. Homer, C. Gerard, and P. W. Noble. 2004. Regulation of pulmonary fibrosis by chemokine receptor CXCR3. *J. Clin. Invest.* 114: 291–299.
33. Bromberg, J. F., C. M. Horvath, X. Wen, R. D. Schreiber, and J. E. Darnell, Jr. 1996. Transcriptionally active STAT-1 is required for the antiproliferative effects of both IFN-α and IFN-γ. *Proc. Natl. Acad. Sci. USA* 93: 7673–7678.
34. Bonner, J. C., A. B. Rice, J. L. Ingram, C. R. Moomaw, A. Nyska, A. Bradbury, A. R. Sessoms, P. C. Chulada, D. L. Morgan, D. C. Zeldin, and R. Langenbach. 2002. Susceptibility of cyclooxygenase (COX)-2 deficient mice to pulmonary fibrosis. *Am. J. Pathol.* 161: 459–470.
35. Khalil, N., and A. H. Greenberg. 1991. The role of TGF-β in pulmonary fibrosis. *Ciba Found. Symp.* 157: 194–207, discussion 207–211.